**Carcinogenesis** vol.32 no.5 pp.772–778, 2011
doi:10.1093/carcin/bgr036
*Advance Access publication February 23, 2011*

# MicroRNA-145 is regulated by DNA methylation and p53 gene mutation in prostate cancer

**Seong O.Suh[1,2,3,†], Yi Chen[1,†], Mohd Saif Zaman[1], Hiroshi Hirata[1], Soichiro Yamamura[1], Varahram Shahryari[1], Jan Liu[1], Z.Laura Tabatabai[2], Sanjay Kakar[2], Guoren Deng[1], Yuichiro Tanaka[1] and Rajvir Dahiya[1,*]**

[1]Department of Urology, Veterans Affairs Medical Center and University of California at San Francisco, San Francisco, CA 94121, USA, [2]Department of Pathology, Veterans Affairs Medical Center and University of California at San Francisco, San Francisco, CA 94121, USA and [3]Department of Internal Medicine, National Police Hospital, Seoul, Korea

[*]To whom correspondence should be addressed. Urology Research Center (112F), Veterans Affairs Medical Center and University of California at San Francisco, 4150 Clement Street, San Francisco, CA 94121, USA.
Tel: +1 415 750 6964; Fax: +1 415 750 6639;
Email: rdahiya@urology.ucsf.edu

**MiR-145 is downregulated in various cancers including prostate cancer. However, the underlying mechanisms of miR-145 downregulation are not fully understood. Here, we reported that miR-145 was silenced through DNA hypermethylation and p53 mutation status in laser capture microdissected (LCM) prostate cancer and matched adjacent normal tissues. In 22 of 27 (81%) prostate tissues, miR-145 was significantly downregulated in the cancer compared with the normal tissues. Further studies on miR-145 downregulation mechanism showed that miR-145 is methylated at the promoter region in both prostate cancer tissues and 50 different types of cancer cell lines. In seven cancer cell lines with miR-145 hypermethylation, 5-aza-2′-deoxycytidine treatment dramatically induced miR-145 expression. Interestingly, we also found a significant correlation between miR-145 expression and the status of p53 gene in both LCM prostate tissues and 47 cancer cell lines. In 29 cell lines with mutant p53, miR-145 levels were downregulated in 28 lines (97%), whereas in 18 cell lines with wild-type p53 (WT p53), miR-145 levels were downregulated in only 6 lines (33%, $P < 0.001$). Electrophoretic mobility shift assay showed that p53 binds to the p53 response element upstream of miR-145, but the binding was inhibited by hypermethylation. To further confirm that p53 binding to miR-145 could regulate miR-145 expression, we transfected WT p53 and MUT p53 into PC-3 cells and found that miR-145 is upregulated by WT p53 but not with MUTp53. The apoptotic cells are increased after WT p53 transfection. In summary, this is the first report documenting that downregulation of miR-145 is through DNA methylation and p53 mutation pathways in prostate cancer.**

## Introduction

Prostate cancer is the most commonly diagnosed cancer among men in the USA. The American Cancer Society estimated that there were 192 280 new cases of prostate cancer and 27 360 deaths in the USA in 2009.

MicroRNAs (miRNAs) are small, non-coding RNA molecules that regulate the expression of protein-coding genes at the translational level. miR-145 was first identified in mouse heart muscle (1) and later was reported in human (2). miR-145 expression is high in germ line and mesoderm-derived tissues such as uterus, ovary, testis, spleen, heart and prostate (3) and plays important roles in the differentiation of stem cells and vascular smooth muscle cells (4,5). miR-145 is a well-known tumor suppressor miRNA, and its expression level is decreased in many human cancers such as breast (6), colon (2), lung (7), liver (8), bladder (9), pituitary (10), B cell (11), ovary (12) and prostate (13–15). miR-145 suppresses tumor cell growth by targeting insulin receptor substrate-1(16), c-Myc (17) and several other genes related to carcinogenesis (18). miR-145 impacts migration, invasion and metastasis by targeting Fli 1 (19) and mucin 1 (20), respectively and also affects p53-mediated cell cycle arrest by targeting p21 (17,21). In addition, downregulation of miR-145 is associated with aggressive phenotype and poor prognosis in prostate cancer (22,23).

In the present study, we explore the expression of miR-145 and its regulation in prostate cancer tissues. Due to the infiltrative feature of most of prostate cancers, tumor cells are scattered within the normal prostate stroma and the tumor content in each tissue is different. Thus, traditionally processed prostate cancer tissues are not representative of cancer cell-specific regulation of miRNA. Therefore, we used laser capture microdissection (LCM) to isolate cancer tissues that were clearly marked by an experienced pathologist. Furthermore, we found that there is a CpG rich regions upstream of the miR-145 gene and previous reports showed that other miRNAs such as miR-127, miR-124a, and miR-34 were downregulated by epigenetic events such as DNA methylation (24,25). Therefore, we investigated methylation status and its effect on miR-145 expression levels. Interestingly, among several CpG sites, two of them flank the p53 response element. It has been previously reported that miR-145 has a p53 response element in its promoter region and its expression level can be induced by p53 at the transcriptional level in breast and colon cancer cell lines (17). Therefore, we hypothesized that miR-145 expression levels are modulated by p53 and the methylation of the promoter region, especially at the p53 response element, may downregulate the expression of miR-145 by inhibiting binding of p53.

**Abbreviations:** BPH, benign prostatic hyperplasia; EMSA, electrophoretic mobility shift assay; FFPE, formalin-fixed, paraffin-embedded; LCM, laser capture microdissected/laser capture microdissection; miRNA, microRNA; PCR, polymerase chain reaction; WT p53, wild-type p53.

[†]These authors contributed equally to this work.

## Materials and methods

### *Tissue samples and cell culture*

Twenty-seven formalin-fixed, paraffin-embedded (FFPE) prostate cancer samples and 25 FFPE benign prostatic hyperplasia (BPH) samples were obtained from the Veterans Affairs Medical Center (San Francisco, CA). Informed consent was obtained from all patients. All slides were reviewed by a board certified pathologist for the identification of prostate cancer foci as well as adjacent normal glandular epithelium. The prostate cancer cell lines LNCaP, DU145, and PC3 were obtained from the American Type Culture Collection (Manassas, VA). The prostate cancer cell lines were grown in RPMI 1640 media (UCSF facility) supplemented with 10% fetal bovine serum (Atlanta biological, Lawrenceville, GA) and 1% penicillin/streptomycin (UCSF facility) and were maintained in an incubator with humidified atmosphere of 95% air and 5% $CO_2$ at 37°C.

The contamination with mycoplasma in cells was tested by polymerase chain reaction (PCR) with e-Myco Plus Mycoplasma PCR Detection Kit (Boca Scientific, Boca Raton, FL). Genomic DNAs (50 ng) of cell lines were added to the tubes containing 1× PCR buffer, deoxynucleoside triphosphates, mycoplasma primers and *Taq* DNA polymerase. PCR was processed according to the procedure recommended by manufacturers. The mycoplasma primers can amplify all important species of mycoplasma including *Mycoplasma opalescens*, *Mycoplasma arginini*, *Mycoplasma fermentans*, *Mycoplasma caviae*, *Mycoplasma hyorhinis*, *Mycoplasma orale* etc. To reduce the chance of false negative, all tubes contain artificial tumor necrosis factor-α gene and its primers as internal control. To test the integrity of DNA samples, a primer set to amplify a housekeeping gene was added to all tubes as sample control. DNA from mycoplasma-contaminated cell line K562 was added to a tube as a positive control. No mycoplasma was contaminated in prostate cancer cell lines PC-3, LNCaP and Du145, kidney cancer cell lines CAKI-2 and A498 and colorectal cancer cell lines C, Colo320, Caco2, HT29, LS174T, RKO and SW48 (supplementary Figure 2 is available at *Carcinogenesis* Online).

© The Author 2011. Published by Oxford University Press. All rights reserved. For Permissions, please email: journals.permissions@oup.com

*Transfection and apoptosis assay*

Cells were placed in six-well plates at 70–90% confluency 24 h before transfection in serum free media. Cells were transfected with various plasmids (2 μg/well) by using Lipofectamine (Invitrogen, Carlsbad, CA) according to the manufacture's protocol. After 72 h, cells were collected by trypsinization, washed with phosphate-buffered saline and dual stained with the viability dye 7-amino-actinomycin D and Annexin V- fluorescein isothiocyanate using Annexin V- fluorescein isothiocyanate /7-amino-actinomyicin D kit (Beckman Coulter, Brea, CA) according to the manufacturer's protocol. Stained cells were immediately analyzed using a flow cytometer (Cell Lab Quanta SC; Beckman Coulter).

*RNA and DNA extraction*

Total RNA was extracted from microdissected FFPE tissue and cultured cells using a miRNeasy FFPE Kit (Qiagen, Valencia, CA) for FFPE tissues and RNeasy mini kit (Qiagen) for cultured cells. Total DNA was extracted from 21 microdissected FFPE prostate cancer tissues and adjacent normal tissues.

*5-Aza-2′-deoxycytidine treatment*

Cells were plated in six-well plates on Day 0, and treated with a final concentration of 5 μM 5-aza-2′-deoxycytidine (Sigma, St Louis, MO) daily beginning from Day 1, until Day 4. The treated cells were harvested on Day 5.

*Quantitative real-time PCR*

Complementary DNAs were synthesized by using specific-miRNA primers (Applied Biosystems, Foster City, CA). Gene expression levels were measured by real-time quantitative PCR using an Applied Biosystems 7500 Fast Sequence Detection and gene-specific Taqman assay kits. RNU48 was used as endogenous control to normalize expression data. The thermal cycling conditions were according to the TaqMan Fast Universal PCR protocol. Each sample was analyzed in quadruplicate.

*Bisulfite modified DNA sequencing*

Methylation status of CpG sites in the miR-145 promoter was determined by $NaHSO_3$-sequencing method. DNA was treated with $NaHSO_3$ and amplified by PCR with the following primer set: forward, 5′GTGTAGATAGTAGAGGGTAGTTT; reverse, 5′TCCCACATCCAACCTCACAAA. This PCR product, which covers the miR-145 promoter region from −224 to +194, was sequenced on an ABI sequencer with dye terminators (Applied Biosystems). The quotient of C over C + T at each CpG site indicates the percentage of methylation.

*Methylation-specific PCR*

The bisulfite-treated genomic DNA was amplified by PCR with a set of primers for the unmethylated reaction and with another set of primers for the methylated reaction: (a) unmethylated forward primer (5′GGGTTTTGGTATTTTTAGGGTAATTGAAGTTTT) and reverse primer (5′AACCAAAATAAAATACCACACATCACCA); (b) methylated forward primer (5′GGGTTTTCGGTATTTTTAGGGTAATTGAAGTTTC) and reverse primer (5′TAAAATACCACACGTCGCCG). PCR was performed at 95°C for 5 min, 40 cycles at 94°C for 30 s, 56°C (unmethylated primer) or 64°C (methylated primer) for 30 s and 72°C for 30 s followed by a final extension at 72°C for 10 min in a PTC-100 thermal cycler (MJ Research, Waltham, MA). The PCR products were loaded on 2.0% agarose gel for analysis.

*Sequence analysis of the p53 gene*

DNA was amplified by PCR using five pairs of primers corresponding to sequences of exons 4–8 of p53 genes (4forward, 5′AAGCTCCCAGAATGCCA and 4reverse, 5′TGAAGTCTCATGGAAGCCAG; 5forward, 5′GTGCCCTGACTTTCAACTCT and 5reverse, 5′CAACCAGCCCTGTCGTCTCT; 6forward, 5′GCCTCTGATTCCTCACTGAT and 6reverse, 5′CCAGAGACCCCAGTTGCAAA; 7forward, 5′CAAGGCGCACTGGCCTCAT and 7reverse, 5′CAGTGTGCAGGGTGGCAAGT and 8forward, 5′GACCTGATTTCCTTACTGCCT and 8reverse, 5′GAATCTGAGGCATAACTGCAC). The PCR product was sequenced on an ABI sequencer with dye terminators (Applied Biosystems).

*Electrophoretic mobility shift assay*

A DNA probe containing the p53 response element at 5′ upstream site (−829 to −810) of miR-145 was obtained by annealing two oligos. A DNA probe containing consensus p53 response element (5′ GCCGAGACATGCCTAGACATGCCTCAA) was obtained by annealing two oligos. EMSA was performed using an EMSA kit (Molecular Probes; Invitrogen) according to the manufacturer's instructions.

*Laser captured microdissection (LCM) and RNA extraction from FFPE human prostate cancer samples*

Microdissection was performed using the AutoPix System from Arcturus. Sections (8 μm) were placed on glass slides, deparaffinized, stained with hematoxylin, dehydrated and placed in the AutoPix instrument for microdissection. Areas of interest were captured with infrared laser pulses onto CapSure Macro LCM Caps (Figure 1).

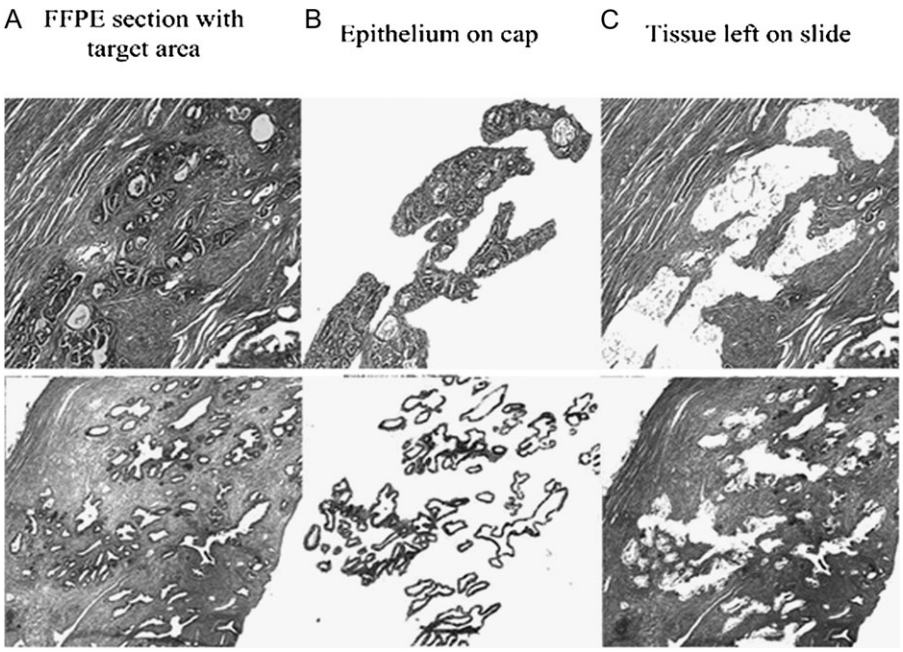


**Fig. 1.** Laser capture microdissection (LCM) in prostate tissues. Upper and lower panels are two prostate tissues. The left panels show targeted glands and stroma before LCM. The center panels show gland cells captured by LCM. The right panels show residual tissues left behind after LCM.

*In situ* hybridization

Non-radioactive *in situ* hybridization was performed on 5 μm sections from FFPE prostate cancer tissue blocks using the digoxigenin-labeled locked nucleic acid modified detection probe (20 μM; 5′-AGGGATTCCTGGGAAAACTGGAC-3′, Exiqon, Tustin, CA) complementary to mature miR-145 and IsHyb in situ hybridization Kit (BioChain, Hayward, CA) following the protocol from Exiqon. Briefly, 5 μm sections were deparaffinized, hydrated, treated with proteinase K (10 μg/ml; Qiagen) at 37°C for 5 min then with 0.2% glycine for 1 min and fixed with 4% paraformaldehyde for 10 min. The sections were incubated in pre-hybridization solution at 50°C for 3 h and then in hybridization solution with digoxigenin -labeled, locked nucleic acid-modified miR145 probe at 57°C for 16 h. The sections were incubated in the phosphate-buffered saline diluted anti- digoxigenin -AP antibody (1:200) at 4°C for 16 h, washed with 2× standard saline citrate, 1.5× standard saline citrate, 0.2× standard saline citrate, incubated in blocking solution for 1 h at room temperature, washed with phosphate-buffered saline three times, then washed with 1× alkaline phosphatase buffer twice. BM purple (Roche South San Francisco, CA) was used for visualization of hybridization signal.

*Statistics*

Statistical analysis was performed with Statview 5.0 for Windows as needed. Wilcoxon signed-rank test was used to compare the matched prostate cancer and adjacent normal samples. The student's t-test was used to compare the different groups. $P$ values $<0.05$ were regarded as statistically significant and are represented by an asterisk on the bars in the figures.

## Results

*The expression of miR-145 in microdissected prostate cancer tissues is lower than the matched adjacent normal regions as well as BPH*

We first examined the expression levels of miR-145 in laser capture microdissected (LCM) prostate cancer tissues and the matched adjacent normal regions by real-time PCR with RNU48 as an internal control. 22/27 (81%) cancer samples showed lower (<75%) miR-145 levels compared with adjacent normal regions, The differences were statistically significant with Wilcoxon signed-rank test ($P < 0.001$) (Figure 2A). In order to compare this result with BPH tissues, we measured miR-145 level in 25 microdissected BPH samples. BPH samples showed significantly higher miR-145 levels compared with 27 pairs of cancer and adjacent normal tissues ($P < 0.001$) (Figure 2B). Furthermore, *in situ* hybridization was performed on prostate cancer tissue and the adjacent normal region. In adjacent normal tissue, we observed a certain amount of blue, irregular dot-shaped staining in epithelial cells, which were lacking or at a much lower

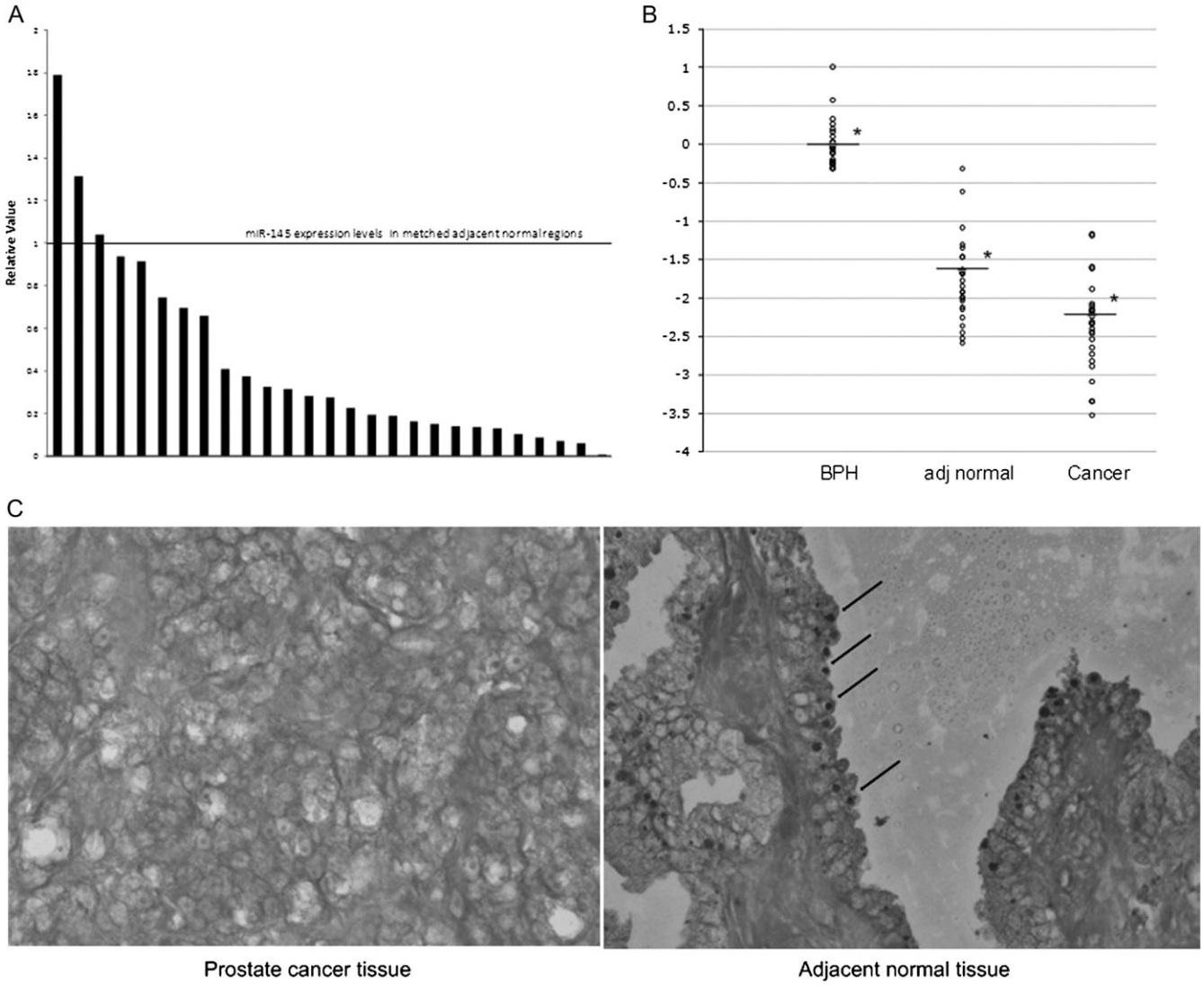


**Fig. 2.** miR-145 expression in prostate cancer, adjacent normal and BPH tissues. (**A**) miR-145 expression determined by qRT-PCR in 27 pairs of prostate cancers and their adjacent normal tissues. (**B**) Expression levels of miR-145 in 25 BPH and 27 pairs of prostate cancer and adjacent normal tissues. (**C**) Loss of miR-145 in prostate cancer determined by locked nucleic acid-*in situ* hybridization (left). miR-145 staining (dark dots, arrowed) can be observed only in the adjacent normal area (right, ×200).

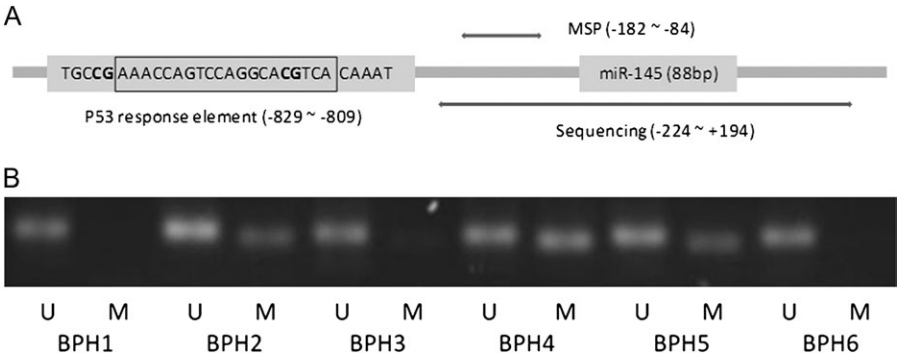


**Fig. 3.** Methylation of miR-145 in prostate cancer, adjacent normal and BPH. (**A**) A schematic description of the putative miR-145 promotor. (**B**) Methylation of miR-145 in BPH samples determined by methylation-specific PCR (U, product from unmethylated primers; M, product from methylated primers).

density in the cancer region, indicating lower expression of miR-145 in adjacent normal tissues compared with the cancer tissues (Figure 2C).

*miR-145 expression in prostate cancers is correlated with p53 status and methylation in the upstream sequence of miR-145 in prostate cancer*

miR-145 contains several CpG sites and p53 response element (Figure 3A). p53 status and methylation in the upstream sequence of miR-145 were examined in 21 prostate cancer and adjacent normal samples. Prostate cancer samples (17 of 21, 81%) showed lower miR-145 expression compared with the adjacent normal regions. In these 17 samples, 6 had both p53 mutations and hypermethylation of miR-145, 5 had only p53 mutations, 3 had only hypermethylation of miR-145, whereas only 3 (18%) had neither p53 mutation nor hypermethylation (Table I, supplementary Figure 1 is available at *Carcinogenesis* Online). In four prostate cancer samples with no downregulation of miR-145, neither p53 mutation nor hypermethylation of miR-145 was detected ($P = 0.022$) (Table I, supplementary Figure 1 is available at *Carcinogenesis* Online). BPH samples (9 of 10) with high expression of miR-145 showed no methylation in the upstream region of miR-145 by methylation-specific PCR. Only one BPH sample showed partial methylation (Figure 3B).

In order to further confirm the correlation of miR-145 level with p53 status and methylation, we measured miR-145 expression levels with p53 status and miR-145 methylation in 47 cancer cell lines, including 4 prostate cancer cell lines, 4 kidney cancer cell lines, 11 breast cancer cell lines, 20 colorectal cancer cell lines and 8 pancreatic cancer cell lines. We observed a significant correlation of miR-145 expression with p53 gene status and miR-145 methylation ($P < 0.001$). In 34 cell lines with low miR-145 expression, 16, 12 and 5 cell lines had both p53 mutations and miR-145 methylation, only p53 mutation, or methylation of miR-145, respectively. p53 mutation and miR-145 methylation were not detected in only one cell line. In 13 cell lines with high miR-145 expression, p53 mutation and miR-145 methylation were not present in 10 cell lines (supplementary Table 1 is available at *Carcinogenesis* Online ).

*5-Aza-2′-deoxycytidine treatment induces the expression of miR-145*

To confirm the silencing effect of miR-145 methylation, seven cancer cell lines with methylated miR-145 promoter (PC3, LNCaP, Du145, HT29, C, Caki2 and A498) and two cell lines with no methylation of miR-145 (SW48, RKO) were treated with DNA methyltransferase inhibitor 5-aza-2′-deoxycytidine. MiR-145 expression was induced in all seven cell lines with methylated miR-145, whereas miR-145 was not as much induced in cell lines with no miR-145 methylation (Figure 4).

*Methylation of miR-145 interferes with the binding of p53 to the p53 response element upstream of miR-145*

To investigate the relationship of methylation and p53 in miR-145 expression, we performed EMSA with a DNA probe containing the p53 response element at the 5′ upstream site (−829 to −810) of miR-145. A band was observed by the binding of probe with LNCaP cell nuclear extract [containing wild-type p53 (WT p53)]. The band was not observed when anti-p53 antibody was added, indicating the nuclear protein was recognized by the anti-p53 antibody. As many investigators showed, in EMSA, the addition of antibodies can lead to either slower mobility of band (supershift) or loss of the shifted band due to the interfering with the formation of protein/DNA complex by the interaction between epitopes and antibodies (http://www.piercenet.com/proteomics, http://www.promega.com/guides). The band was not formed when the methylated probe was mixed with LNCaP cell nuclear extract (Figure 5A), indicating that methylation of the miR-145 promoter region interferes with p53 binding. To confirm the shifted band is the complex of p53 and p53 element in miR-145 promoter, we performed EMSA with a probe of consensus p53 response element (Figure 5B). The band was shifted as in Figure 5A,

**Table I.** Correlation of miR-145 expression levels with p53 status and miR-145 methylation in tumor and adjacent normal tissues

| Samples | miR-145 expression | Met-T (%) | Met-N (%) | dMet (T-N) | p53 mutation |
|---|---|---|---|---|---|
| 1 | **0.224** | 98 | 60 | **38** | S241F |
| 2 | **0.087** | 78 | 60 | 18 | N288Y |
| 3 | **0.141** | 71 | 26 | **45** | C242S |
| 4 | **0.744** | 80 | 75 | 5 | R175P |
| 5 | 1.316 | 69 | 67 | 2 | — |
| 6 | **0.192** | 87 | 60 | **27** | Y236N |
| 7 | **0.103** | 93 | 58 | **35** | M246L |
| 8 | **0.694** | 88 | 64 | **24** | — |
| 9 | **0.130** | 87 | 83 | 4 | — |
| 10 | 0.938 | 86 | 81 | 5 | — |
| 11 | 1.038 | 76 | 71 | 5 | — |
| 12 | 0.913 | 93 | 82 | 11 | — |
| 13 | **0.276** | 86 | 62 | **24** | S240G |
| 14 | **0.191** | 83 | 79 | 4 | A119T |
| 15 | **0.061** | 83 | 60 | **23** | — |
| 16 | **0.407** | 77 | 69 | 8 | — |
| 17 | **0.375** | 74 | 58 | 16 | C242Y |
| 18 | **0.008** | 85 | 63 | **22** | — |
| 19 | **0.163** | 86 | 60 | **26** | Q104E |
| 20 | **0.326** | 77 | 73 | 4 | — |
| 21 | **0.658** | 89 | 76 | 13 | R273S |

Low miR-145 expression was arbitrarily defined as smaller than 0.75 (standardized by adjacent normal) and indicated in bold. Methylation (%) in tumor (T) and adjacent normal (N) was the average of percentages at six CpG sites. dMethylation was the difference between methylation in cancer and adjacent normal. Values >20 were considered to represent significantly higher methylation and shown in bold. p53 mutations are indicated with codon number and names of involved amino acids.

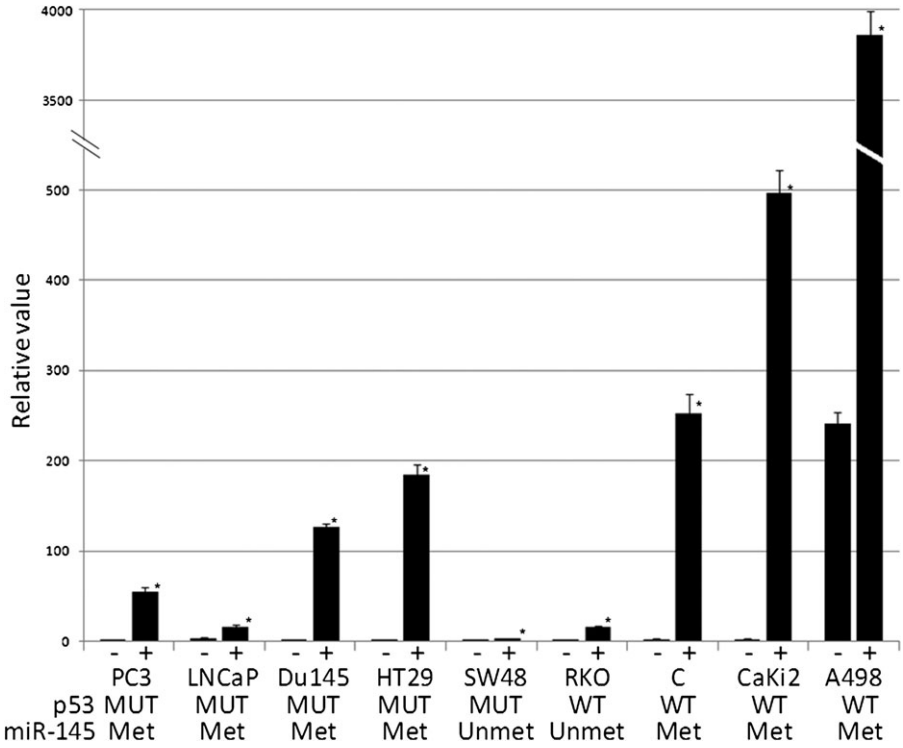


**Fig. 4.** MiR-145 levels were upregulated by 5-aza-2′-deoxycytidine treatment. P53 status and methylation of miR-145 promoter region is shown below each cell line name. In each cell line, left bar is the untreated control.

and the shifted band was not observed when anti-p53 antibody was added. The methylation also interfered with the formation of protein/DNA complex as in Figure 5A.

*Increase in miR-145 expression and apoptotic cells after transfection of PC-3 cells with WT p53 plasmid but not with mutant p53 (MUT p53)*

To check if miRNA-145 is regulated by p53 and if there is any biological alteration in cells, PC-3 cells were transfected with either WT P53 or MUT P53-expressing plasmids. MiR-145 levels were measured by real-time PCR 72 h after transfection. pCMV vector which does not contain any p53 sequence was used as a control. miR-145 was induced ∼30–40% after PC-3 cells were transfected with WT p53. However, no induction was observed in the MUT p53-transfected samples (Figure 5C). Apoptosis analysis was performed 72 h after the transfection. The apoptotic cells were significantly increased in the cells transfected with WT p53 (12.72%) as compared with the cells transfected with MUT p53 (5.59%) (Figure 5D). These results indicate that WT p53 binding to the p53 response element upstream of miR-145 can upregulate the transcription of miR-145 and increase apoptosis in PC-3 cells and the wild-type sequence of p53 is critical to its regulation.

## Discussion

Prostate cancer is a slow growing male reproductive system malignant tumor. In most cases, prostate cancers are infiltrative and tumor cells are scattered within the normal prostate stroma, making the tumor content in each sample quite different. Therefore obtaining pure cancer cells for analysis is very difficult and critical. Laser capture microdissection (LCM) has been considered as a useful tool for distinguishing cancer cells from the background stroma or adjacent normal tissues. In our present study, we used laser capture microdissected prostate tissues to analyze miR-145 expression levels and real-time PCR showed that it was downregulated in prostate cancer compared with adjacent normal tissues. Our observation is consistent with previous reports about the miR-145 expression levels in prostate (13–15,23), although none of these studies used microdissected tissues. In addition, our data showed that miR-145 expression level was decreased in adjacent normal tissue compared with that of BPH (noncancerous prostate hypertrophy). This could be explained by the cancer field effect, which has been characterized as the occurrence of multiple genetic and epigenetic changes in normal tissues adjacent to cancers (26–28). Michael *et al*. (2) also reported decreased miR-145 levels in both colon cancers and adenomatous polyps compared with normal colon tissues. Decreased miR-145 levels in precancerous lesions and adjacent tumor tissues suggest that miR-145 might play a role in prostate cancer initiation.

To explore the mechanism of miR-145 downregulation in prostate cancers, we first investigated the promoter methylation status of miR-145. DNA methylation, as one of the important gene silencing mechanisms, can occur at repetitive sequences, retroelements and genes. The target sequences are methylated by DNA methyltransferases and are characterized by a comparatively high density of CpG dinucleotides (29). It has been reported that DNA methylation downregulates the expression of miRNAs such as miR-127, miR-124a and miR-34 (24). Approximately half of all known human miRNA genes are associated with CpG islands (29). Our data showed that 9 of 21 cancer tissues had a significantly higher (20% more than adjacent normal tissues) methylation rate, and all nine samples showed lower expression of miR-145 compared with adjacent normal tissues.

Interestingly, previous reports have also shown co-operative action of p53 and methylation in miRNA regulation. For example, miR-34 which is directly transactivated by p53 was also reported to be downregulated by methylation (30,31). Therefore, we looked at the p53 status and relationship with miR-145 expression level in prostate tissue samples. It is known that p53 regulates many genes at the transcriptional level by binding to specific-DNA sequences. Somatic p53 missense mutations are found in ∼50% of human cancers (32). In prostate cancer, p53 mutation is correlated with high-grade,

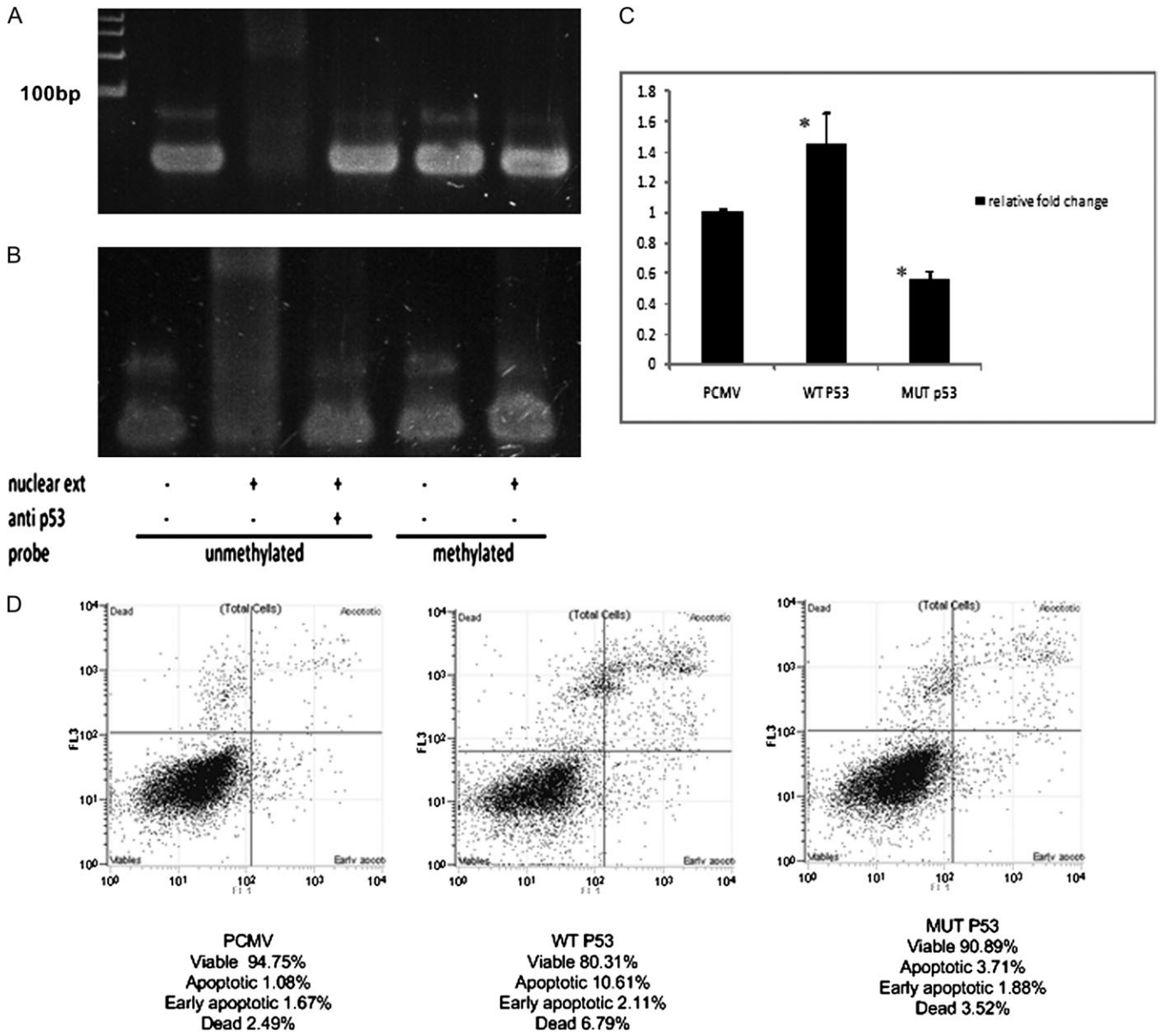


**Fig. 5.** WT p53 binds to miR-145 promoter, regulates its expression and increases apoptosis of cells. (**A**) The binding of p53 to the p53 response element upstream of miR-145 gene shown by EMSA. The binding of p53 to the p53 response element is indicated by the arrow. (**B**) The binding of p53 to the consensus p53 response element shown by EMSA. The binding of p53 to the p53 response element is indicated by the arrow. (**C**) miR-145 expression levels are up regulated after transfection of PC-3 cells with WT p53 but not mutant p53 by real-time PCR. Empty vector pCMV was used as a control. (**D**) Apoptotic cells are significantly increased after transfection of PC-3 cells with WT p53 (12.72%), but not with MUT p53 (5.59%). Empty vector pCMV is used as a control (2.75%).

high-stage tumors and poor prognosis (33). Multiple miRNAs have been reported as being components of p53/p63 networks and were regulated by p53 (34,35). Sachdeva *et al*. (17) reported p53 response element on the miR-145 promoter sequence and proved its function in breast and colon cancer cell lines. In our study, 10 of 21 (47.6%) tissue samples showed p53 mutation in exons 4–8, all of which had low miR-145 expression level compared with adjacent normal regions, suggesting p53 can regulate miR-145 expression levels. EMSA studies with the p53 response element in the miR-145 promoter region also confirmed that p53 can bind to miR-145 and possibly regulate its expression. However, no significant correlation between p53 mutation and tumor grade or stage was found. In addition, methylation altered the binding affinity of the p53 response element (36). In our study, we also observed that only unmethylated DNA probe bound to LNCaP cell nuclear extract containing WT p53, suggesting a co-operative role of methylation with p53 mutation.

Our present study found that only a small number of tissues and cell lines had low miR-145 expression levels without p53 mutation or methylation, which could be explained by the existence of p53 mutations other than exons 4–8 (5%) (32) or other mechanisms such as posttranslational regulation of p53 by MDM2 (37,38).

In summary, our results suggest that methylation of the promoter region of miR-145 in both cell lines and carcinoma samples are a major reason for its low expression. This is the first report on the mechanisms of regulation of miR-145 through DNA methylation and p53 gene mutation, thus making miR-145 an important therapeutic target for the management of prostate cancer.

## Supplementary material

Supplementary Table 1 and Figures 1 and 2 can be found at http://carcin.oxfordjournals.org/

## Funding

National Institutes of Health (RO1CA138642–01, T32DK007790); Research Enhancement Award Program for prostate cancer and Veterans Affairs Merit Review.

## Acknowledgements

We thank Dr Roger Erickson for his support and assistance with the preparation of the manuscript.

*Conflict of Interest Statement:* None declared.

## References

1. Lagos-Quintana,M. *et al*. (2001) Identification of novel genes coding for small expressed RNAs. *Science*, **294**, 853–858.
2. Michael,M.Z. *et al*. (2003) Reduced accumulation of specific microRNAs in colorectal neoplasia. *Mol. Cancer Res.*, **1**, 882–891.
3. Lakshmipathy,U. *et al*. (2007) Micro RNA profiling: an easy and rapid method to screen and characterize stem cell populations. *Methods Mol. Biol.*, **407**, 97–114.
4. Cordes,K.R. *et al*. (2009) miR-145 and miR-143 regulate smooth muscle cell fate and plasticity. *Nature*, **460**, 705–710.
5. Xu,N. *et al*. (2009) MicroRNA-145 regulates OCT4, SOX2, and KLF4 and represses pluripotency in human embryonic stem cells. *Cell*, **137**, 647–658.
6. Iorio,M.V. *et al*. (2005) MicroRNA gene expression deregulation in human breast cancer. *Cancer Res.*, **65**, 7065–7070.
7. Liu,X. *et al*. (2009) Uncovering growth-suppressive microRNAs in lung cancer. *Clin. Cancer Res.*, **15**, 1177–1183.
8. Gramantieri,L. *et al*. (2009) MicroRNA-221 targets Bmf in hepatocellular carcinoma and correlates with tumor multifocality. *Clin. Cancer Res.*, **15**, 5073–5081.
9. Ichimi,T. *et al*. (2009) Identification of novel microRNA targets based on microRNA signatures in bladder cancer. *Int. J. Cancer*, **125**, 345–352.
10. Amaral,F.C. *et al*. (2009) MicroRNAs differentially expressed in ACTH-secreting pituitary tumors. *J. Clin. Endocrinol. Metab.*, **94**, 320–323.
11. Akao,Y. *et al*. (2007) Downregulation of microRNAs-143 and -145 in B-cell malignancies. *Cancer Sci.*, **98**, 1914–1920.
12. Iorio,M.V. *et al*. (2007) MicroRNA signatures in human ovarian cancer. *Cancer Res.*, **67**, 8699–8707.
13. Porkka,K.P. *et al*. (2007) MicroRNA expression profiling in prostate cancer. *Cancer Res.*, **67**, 6130–6135.
14. Ozen,M. *et al*. (2008) Widespread deregulation of microRNA expression in human prostate cancer. *Oncogene*, **27**, 1788–1793.
15. Schaefer,A. *et al*. (2010) Diagnostic and prognostic implications of microRNA profiling in prostate carcinoma. *Int. J. Cancer*, **126**, 1166–1176.
16. Shi,B. *et al*. (2007) Micro RNA 145 targets the insulin receptor substrate-1 and inhibits the growth of colon cancer cells. *J. Biol. Chem.*, **282**, 32582–32590.
17. Sachdeva,M. *et al*. (2009) p53 represses c-Myc through induction of the tumor suppressor miR-145. *Proc. Natl Acad. Sci. USA*, **106**, 3207–3212.
18. Sachdeva,M. *et al*. (2010) miR-145-mediated suppression of cell growth, invasion and metastasis. *Am. J. Transl. Res.*, **2**, 170–180.
19. Larsson,E. *et al*. (2009) Discovery of microvascular miRNAs using public gene expression data: miR-145 is expressed in pericytes and is a regulator of Fli1. *Genome Med.*, **1**, 108.
20. Sachdeva,M. *et al*. (2010) MicroRNA-145 suppresses cell invasion and metastasis by directly targeting mucin 1. *Cancer Res.*, **70**, 378–387.
21. Seoane,J. *et al*. (2002) Myc suppression of the p21(Cip1) Cdk inhibitor influences the outcome of the p53 response to DNA damage. *Nature*, **419**, 729–734.
22. Wang,L. *et al*. (2009) Gene networks and microRNAs implicated in aggressive prostate cancer. *Cancer Res.*, **69**, 9490–9497.
23. Chen,X. *et al*. (2010) MicroRNA145 targets BNIP3 and suppresses prostate cancer progression. *Cancer Res.*, **70**, 2728–2738.
24. Lujambio,A. *et al*. (2007) CpG island hypermethylation of tumor suppressor microRNAs in human cancer. *Cell Cycle*, **6**, 1455–1459.
25. Corney,D.C. *et al*. (2010) Frequent downregulation of miR-34 family in human ovarian cancers. *Clin. Cancer Res.*, **16**, 1119–1128.
26. Chandran,U.R. *et al*. (2005) Differences in gene expression in prostate cancer, normal appearing prostate tissue adjacent to cancer and prostate tissue from cancer free organ donors. *BMC Cancer*, **5**, 45.
27. Mehrotra,J. *et al*. (2008) Quantitative, spatial resolution of the epigenetic field effect in prostate cancer. *Prostate*, **68**, 152–160.
28. Yu,Y.P. *et al*. (2004) Gene expression alterations in prostate cancer predicting tumor aggression and preceding development of malignancy. *J. Clin. Oncol.*, **22**, 2790–2799.
29. Weber,B. *et al*. (2007) Methylation of human microRNA genes in normal and neoplastic cells. *Cell Cycle*, **6**, 1001–1005.
30. Lodygin,D. *et al*. (2008) Inactivation of miR-34a by aberrant CpG methylation in multiple types of cancer. *Cell Cycle*, **7**, 2591–2600.
31. Toyota,M. *et al*. (2008) Epigenetic silencing of microRNA-34b/c and B-cell translocation gene 4 is associated with CpG island methylation in colorectal cancer. *Cancer Res.*, **68**, 4123–4132.
32. Soussi,T. *et al*. (2006) Locus-specific mutation databases: pitfalls and good practice based on the p53 experience. *Nat. Rev. Cancer*, **6**, 83–90.
33. Dong,J.T. (2006) Prevalent mutations in prostate cancer. *J. Cell. Biochem.*, **97**, 433–447.
34. Hermeking,H. (2007) p53 enters the microRNA world. *Cancer Cell*, **12**, 414–418.
35. Barlev,N.A. *et al*. (2010) The microRNA and p53 families join forces against cancer. *Cell Death Differ.*, **17**, 373–375.
36. Hanafusa,T. *et al*. (2005) Functional promoter upstream p53 regulatory sequence of IGFBP3 that is silenced by tumor specific methylation. *BMC Cancer*, **5**, 9.
37. Haupt,Y. *et al*. (1997) Mdm2 promotes the rapid degradation of p53. *Nature*, **387**, 296–299.
38. Kubbutat,M.H. *et al*. (1997) Regulation of p53 stability by Mdm2. *Nature*, **387**, 299–303.

*Received June 2, 2010; revised February 6, 2011; accepted February 17, 2011*